

## Solid Solutions $\text{Ca}_3\text{Sn}_{2+x}\text{Si}(\text{Ge})_{1-x}\text{Ga}_2\text{O}_{12}$ ( $0 \leq x \leq 0.95$ ) and Tetrahedral Coordination of $\text{Sn}^{4+}$ in the Garnet Structure

A. RULMONT AND P. TARTE

*University of Liège, Institute of Chemistry, B-4000 Sart Tilman par Liège 1, Belgium*

AND B. CARTIÉ AND J. CHOISNET

*Centre de Recherches sur la Matière Divisée, Unité mixte CNRS-Université d'Orléans—Cristallochimie, Faculté des Sciences, Université d'Orléans, F-45067 Orléans Cedex 2, France*

Received May 7, 1992; in revised form September 23, 1992; accepted September 24, 1992

Pure solid solutions  $\text{Ca}_3\text{Sn}_{2+x}\text{Si}(\text{Ge})_{1-x}\text{Ga}_2\text{O}_{12}$  with the garnet structure have been evidenced in the composition range  $0 \leq x \leq 0.95$ . This implies that a part of the  $\text{Sn}^{4+}$  cations (equal to  $x$ ) is located on the tetrahedral sites, a quite unusual coordination for this cation in oxygen compounds. This has been definitely confirmed by X-ray powder diffraction structure calculations. Information about the cation-oxygen distances and the distortion of the different coordinated groups is presented. No band characteristic of the  $\text{SnO}_4$  tetrahedra is observed in the IR spectrum, probably because of a strong mixing between  $\text{SnO}_4$  and  $\text{GaO}_4$  vibrations. In contrast, the totally symmetric stretching mode  $\nu_1$  of the  $\text{SnO}_4$  tetrahedra is easily observed near  $775 \text{ cm}^{-1}$  in the Raman spectrum, where it is well separated from the corresponding mode of the  $\text{GaO}_4$  tetrahedra. The different vibrational behavior observed in IR and Raman spectra is discussed on the basis of the symmetry properties of the vibrations. © 1993 Academic Press, Inc.

### Introduction

Tetrahedral coordination of tin(IV) in its oxygen compounds may be considered as exceptional. It has been evidenced in the stannates  $M_1^I\text{SnO}_4$  ( $M^I = \text{Na}, \text{K}$ ) (1) and, quite recently, in solid solutions with the garnet structure in the pseudoquaternary system  $\text{CaO}-\text{Fe}_2\text{O}_3-\text{TiO}_2-\text{SnO}_2$  (2). It should also be present in a garnet " $\text{Ca}_3\text{Sn}_3\text{Ga}_2\text{O}_{12}$ " discovered by Mill' (3), but whose true composition is possibly slightly different from the proposed ideal formula (4).

Because of this uncertainty, and also because of the interest of such a composition for a study of the vibrational behavior of the  $(\text{SnO}_4)$  group, we have investigated the formation of pure garnet phases in the sys-

tems  $\text{Ca}_3\text{Sn}_{2+x}\text{Si}_{1-x}\text{Ga}_2\text{O}_{12}$  and  $\text{Ca}_3\text{Sn}_{2+x}\text{Ge}_{1-x}\text{Ga}_2\text{O}_{12}$  whose first end-members ( $x = 0$ ) are pure garnets, the second end-member ( $x = 1$ ) being the compound under discussion.

### Experimental

*Synthesis of the compounds.* All compounds and solid solutions were prepared by conventional solid state reaction techniques, starting from the stoichiometric quantities of  $\text{CaCO}_3$ ,  $\text{SnO}_2$ ,  $\text{SiO}_2$  (aerosil) or  $\text{GeO}_2$ , and  $\text{Ga}_2\text{O}_3$ .

The mixture is heated in covered Pt crucibles, first to  $900^\circ\text{C}$ , and then by steps of  $100^\circ\text{C}$  with intervening mixing and grinding up to  $1300^\circ\text{C}$ ; this temperature is maintained for one or several days with repeated grind-

ings, until no change is observed in the X-ray diffraction pattern. The full synthesis procedure was repeated two or three times for some compositions containing a small amount of impurity.

**X-ray powder diffraction.** For the phase analysis and cell parameter determination, powder diagrams were recorded with a CGR diffractometer,  $\text{CoK}\alpha$  radiation. Unit cell parameters (accurate to 0.001 Å) were deduced from high-angle diffraction peaks (up to  $75^\circ \theta$ ) corresponding to the (10.4.0), (10.4.2), (8.8.0), (12.0.0), (12.2.2), (12.6.0), and (12.6.2) reflections. As regards structure calculations, diffractograms were recorded up to  $100^\circ 2\theta$  on a Siemens D 500 diffractometer,  $\text{CuK}\alpha$  radiation.

**Vibrational spectroscopy.** The infrared spectra were recorded with a Beckman 4250 infrared spectrometer ( $1400\text{--}300\text{ cm}^{-1}$ , KBr discs) and a Polytec FIR 30 interferometer ( $350\text{--}30\text{ cm}^{-1}$  polyethylene discs). The Raman spectra were recorded with a Coderg PHO double monochromator equipped with an  $\text{Ar}^+$  laser; most spectra were recorded with a slit width of about  $3\text{ cm}^{-1}$ , with a laser power of 200 mW on the 514.5-nm green line.

## Results

### Reproducibility of the Syntheses

Some difficulties were experienced in obtaining pure phases with the  $\text{SnO}_2$ -rich compositions, the main impurity being a small quantity of  $\text{CaSnO}_3$ , easily evidenced by X-ray diffraction (and also appearing in the Raman spectrum). In these cases, the full synthesis process (starting again from the initial mixture of oxides and carbonates) was repeated two or three times, and it was generally possible to obtain  $\text{CaSnO}_3$ -free solid solutions. We suspect this problem of nonreproducibility to be of kinetic origin: once formed,  $\text{CaSnO}_3$  (which is a very stable perovskite) reacts very slowly with the remaining reactants or intermediate products, and it is very difficult to get rid of the last parts of this impurity. Despite repeated ex-

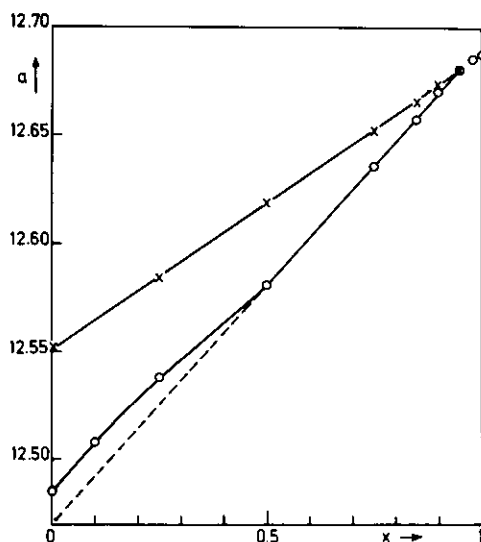


FIG. 1. Variation of the unit cell parameter of the garnet phase as a function of the Si-Sn (circles) or Ge-Sn (crosses) replacement in the solid solutions  $\text{Ca}_3\text{Sn}_{2+x}\text{Si}_{1-x}\text{Ga}_2\text{O}_{12}$ .

periments, we were unable to obtain  $\text{CaSnO}_3$ -free phases for the  $\text{SnO}_2$ -richest compositions, corresponding to  $x = 0.98$  and  $x = 1$ . Thus, the existence of a pure garnet  $\text{Ca}_3\text{Sn}_3\text{Ga}_2\text{O}_{12}$  is doubtful, in agreement with Geller's results (4).

### X-Ray Diffraction

**Cell parameters.** The values of the  $a_0$  parameter for all investigated compositions are plotted in Fig. 1.

$\text{Ca}_3\text{Sn}_{2+x}\text{Si}_{1-x}\text{Ga}_2\text{O}_{12}$ : A linear relationship between  $a_0$  and  $x$  is observed in the composition range  $0.5 \leq x \leq 0.95$ , namely the Sn-rich solid solutions; but for increasing amounts of Si ( $0.5 \geq x \geq 0$ ), the relationship exhibits a positive deviation, the unit cell parameter being greater than expected from the extrapolated initial straight line.

As a consequence of the large difference between the ionic radii of  $\text{Si}^{4+}$  (0.26 Å) and  $\text{Ga}^{3+}$  (0.47 Å) or  $\text{Sn}^{4+}$  (0.55 Å) (5), one can assume some nonstatistical trend in the cationic distribution, in terms of a segregation of  $\text{Si}^{4+}$ -rich microdomains.

TABLE I  
 ATOMIC PARAMETERS FOR THE GARNET TYPE STRUCTURE OF THE SOLID SOLUTIONS  
 $\text{Ca}_3\text{Sn}_{2+x}\text{Si}_{1-x}\text{Ga}_2\text{O}_{12}$  ( $x = 0.0, 0.05, 0.95$ )

Composition ( $x$ value)	Oxygen sites (96 $h$ )			$B(\text{\AA})^2$
	$x$	$y$	$z$	
0.0	0.962(1)	0.050(1)	0.157(1)	1.8(3)
0.05	0.963(2)	0.049(1)	0.155(1)	2.1(2)
0.95	0.966(2)	0.048(1)	0.153(1)	1.0(2)
Isotropic thermal factors of cations				
Composition ( $x$ value)	CN VIII site $\text{Ca}^{2+}$ $B(\text{\AA})^2$	CN VI site $\text{Sn}^{4+}$ $B(\text{\AA})^2$	CN IV site $\text{Ga}^{3+}, \text{Si}^{4+}, \text{Sn}^{4+}$ $B(\text{\AA})^2$	
0.0	0.9(1)	0.2(1)	0.6(2)	
0.05	0.8(1)	0.2(1)	0.5(2)	
0.95	0.6(1)	0.5(1)	0.5(1)	
$\text{RI} = \frac{\sum  I_o - I_c }{\sum I_o}$	$x = 0.0$	(1) 0.040	(2) 0.061	
	$x = 0.05$		0.038	0.064
	$x = 0.95$		0.042	0.078

(1) calculated from the observed reflections

(2) calculated from the whole possible reflections (see text)

For  $x = 0.98$  and 1, there is a weak, downward curvature suggesting that the increase of the  $a_0$  parameter with  $x$  is smaller than expected from the main curve. This is probably correlated with the fact that it was impossible to obtain these two compositions completely free from  $\text{CaSnO}_3$ , thus suggesting that, for these last garnets, the true composition is slightly different from the nominal one. Geller (4) had already noticed the existence of very weak extra lines in the X-ray powder diagram of  $\text{Ca}_3\text{Sn}_3\text{Ga}_2\text{O}_{12}$ . For this composition, we find  $a_0 = 12.687 \text{ \AA}$ , in good agreement with the values proposed either by Mill' (3) (12.69  $\text{\AA}$ ) or by Geller (4) (12.685  $\text{\AA}$ ).

$\text{Ca}_3\text{Sn}_{2+x}\text{Ge}_{1-x}\text{Ga}_2\text{O}_{12}$ . The experimental results suggest a practically linear relationship between the unit cell parameter  $a_0$  and the substitution rate  $x$ , since the very small observed deviations have no systematic character. This behavior is rather different from that observed with the Si-bearing solid

solutions, but this is not unexpected in view of the larger difference between the ionic radii of the tetracoordinated  $\text{Si}^{4+}$  (0.26  $\text{\AA}$ ) and  $\text{Sn}^{4+}$  (0.55  $\text{\AA}$ ) cations (to be compared with the ionic radius of 0.39  $\text{\AA}$  for  $\text{Ge}^{4+}$ ). In any case, the most important point of these results is the conclusion that, for  $x$  values up to 0.95 (namely the range of pure garnet solid solutions), a part of  $\text{Sn}^{4+}$ , equal to  $x$ , is necessarily located on the tetrahedral sites.

*Structure calculations.* In order to check some structural characteristics related to the simultaneous presence of  $\text{Sn}^{4+}$  in octahedral and tetrahedral coordination, calculations from integrated intensities of X-ray diffractograms were undertaken.

Two kinds of calculations (6) were systematically performed:

(i) by using 22 observed reflections, with or without superpositions, i.e., 27  $hkl$  up to 100  $2\theta$ ;

(ii) by including the nonobserved reflections which are possible in the space group

TABLE II  
 ( $M-O$ ) AND ( $O-O$ ) DISTANCES ( $\text{\AA}$ ) FOR THE POLYHEDRA OF THE GARNET TYPE STRUCTURE OF THE SOLID SOLUTIONS  $\text{Ca}_3\text{Sn}_{2+x}\text{Si}_{1-x}\text{Ga}_2\text{O}_{12}$  ( $x = 0.0, 0.05, 0.95$ ).

		$x = 0.0$	$x = 0.05$	$x = 0.95$
( $M-O_4$ ) tetrahedra, $M = \text{Ga}^{3+}, \text{Si}^{4+}, \text{Sn}^{4+}$				
( $M-O$ )	4 $\times$	1.70(1)	1.73(1)	1.79(1)
( $O-O$ )I	2 $\times$	2.63(2)	2.66(3)	2.74(3)
( $O-O$ )I'	4 $\times$	2.85(2)	2.89(3)	3.01(3)
( $M-O_6$ ) octahedra, $M = \text{Sn}^{4+}$				
( $M-O$ )	6 $\times$	2.11(1)	2.09(1)	2.08(1)
( $O-O$ )II	6 $\times$	2.99(2)	2.95(3)	2.91(3)
( $O-O$ )II'	6 $\times$	2.98(2)	2.95(3)	2.97(3)
( $M-O_8$ ) dodecahedra, $M = \text{Ca}^{2+}$				
( $M-O$ )	4 $\times$	2.43(2)	2.42(3)	2.44(3)
( $M-O$ )	4 $\times$	2.57(2) } $\sim 2.50$	2.58(3) } $\sim 2.50$	2.62(3) } $\sim 2.53$
( $O-O$ )I	2 $\times$	2.63(2)	2.66(3)	2.74(3)
( $O-O$ )II	4 $\times$	2.99(2)	2.95(3)	2.91(3)
( $O-O$ )III	2 $\times$	2.96(2)	2.99(3)	3.09(3)
( $O-O$ )IV	4 $\times$	2.98(2)	3.00(3)	3.05(3)

Note. ( $O-O$ ) (I) and (II): shared between tetrahedra (octahedra) and dodecahedra. ( $O-O$ ) (IV): shared between two dodecahedra. ( $O-O$ )I', ( $O-O$ ) II', ( $O-O$ ) III: unshared.

and giving them an intensity equal to 1% of the highest observed intensity: the total number of reflections is 46, i.e., 68  $hkl$ .

Owing to the greater difference between the scattering factors of Si and Sn, the Si-bearing solid solutions  $\text{Ca}_3\text{Sn}_{2+x}\text{Si}_{1-x}\text{Ga}_2\text{O}_{12}$  (compositions  $x = 0, 0.05$  and  $0.95$ ) were preferred. The usual model of the garnet type structure was used, namely space group  $Ia3d$ ;

$\text{Ca}^{2+}$ , coordination VIII, site 24(c):  $\frac{1}{8}, 0, \frac{1}{4}$   
 $\text{Sn}^{4+}$ , coordination VI, site 16(a):  $0, 0, 0$   
 ( $\text{Ga}^{3+}, \text{Si}^{4+}, \text{Sn}^{4+}$ ), coordination IV, site 24(d):  $\frac{3}{8}, 0, \frac{1}{4}$

$\text{O}^{2-}$ , coordination IV, site 96(h):  $x = 0.96$ ,  
 $y = 0.05, z = 0.15$ .

Table I reports the values of oxygen atomic parameters and isotropic thermal factors of both cations and oxygen, obtained after a least-squares refinement procedure. In any case, satisfactory results are observed: RI confidence factors close to 0.04; RI confidence factors calculated for the whole set of possible reflections up to  $100^\circ 2\theta$  in the range 0.06–0.08; values of oxygen atomic

parameters slightly varying; isotropic thermal factors at the octahedral and tetrahedral sites of the right order of magnitude— $0.2 \leq B \leq 0.5 \text{ \AA}^2$ —though the small differences between individual cations are not significant.

The  $M-O$  and  $O-O$  distances at the three cationic sites are listed in Table II. The main feature to be emphasized is the rather strong increase of the ( $M-O$ )<sup>IV</sup> distance in the tetrahedral sites, as a result of the  $\text{Si} \rightarrow \text{Sn}$  replacement: the difference  $\Delta (M-O)^{\text{IV}} x: 0 \rightarrow 0.95$  is close to  $0.09 \text{ \AA}$ , this being fully consistent with the prediction from ionic radii:  $\frac{1}{3} (r(\text{Sn}^{4+})^{\text{IV}} - r(\text{Si}^{4+})^{\text{IV}}) \approx 0.10 \text{ \AA}$ . Otherwise, the ( $\text{Sn}^{4+}-\text{O}$ )<sup>VI</sup> distances in the octahedral sites, as well as the ( $\text{Ca}^{2+}-\text{O}$ )<sup>VIII</sup> distances, are only slightly modified when  $\text{Sn}^{4+}$  enters the tetrahedral sites.

Because of the lack of data for tetrahedrally coordinated  $\text{Sn}^{4+}$  in oxides (such data did not exist up to now for the garnet type structure), any precise discussion in this respect is precluded. Nevertheless, we propose in the following a discussion of crystal

chemical trends, in terms of the regularity or possible distortions of polyhedra, a matter of significant interest with numerous data reported up to now (4, 7, 8). We deal with two points successively: the cooperative distortions of octahedra and tetrahedra, and then the cooperative distortions of tetrahedra and eight-coordinated sites.

(i) Cooperative distortions of octahedra and tetrahedra: From the data of Table II, it can be stated that  $(\text{SnO}_6)$  octahedra are nearly regular, as their trigonal distortion is very low: the difference between the two sets of six (O–O) values  $\Delta(\text{O–O})_{6,6}$  does not exceed  $0.06 \text{ \AA}$ . Conversely, the  $(\text{MO}_4)$  tetrahedra, including or not including  $\text{Sn}^{4+}$  ions, exhibit a rather strong axial distortion resulting in a large value of  $\Delta(\text{O–O})_{2,4}$ :  $0.22 \text{ \AA} \leq \Delta(\text{O–O})_{2,4} \leq 0.27 \text{ \AA}$ . This result is in full agreement with the usual trend of the garnet type structure, in terms of the likely impossibility of getting simultaneously a high regularity of both tetrahedra and octahedra (7). Such a situation has been proved to result in an excessive lowering of the two unshared (O–O)<sub>III</sub> edges of the eight-coordinated site (8). As a consequence, it can be stated that cooperative distortions of octahedra and tetrahedra do not occur directly, but by means of eight-coordinated sites which share edges either with octahedra or with tetrahedra (see Fig. 2).

(ii) Cooperative distortions of tetrahedra and eight-coordinated sites: The  $(\text{M–O})^{\text{IV}}$  distances observed for the Si-bearing solid solutions are systematically smaller than predicted from ionic radii:  $1.70 \rightarrow 1.79 \text{ \AA}$  against  $1.80 \rightarrow 1.89 \text{ \AA}$ . At the same time, the  $(\text{Ca–O})^{\text{VIII}}$  distances nearly fit the theoretical value  $2.52 \text{ \AA}$ . The simultaneous existence of these two data seems to be unusual: generally speaking, the  $(\text{M–O})^{\text{IV}}$  distances are very close to the theoretical values, as observed, for example, in numerous  $\text{Ca}^{2+}$  garnet type silicates, but simultaneously, a significant negative deviation, often close to  $0.10 \text{ \AA}$ , exists for the  $(\text{Ca–O})^{\text{VIII}}$  distance (7, 8). From this, one can consider our own data to be another example of a cooperative

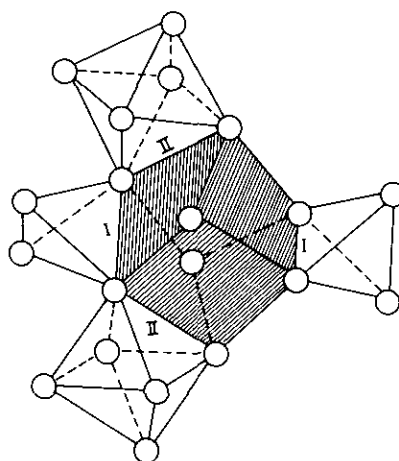


FIG. 2. The distorted dodecahedron (hatched) of the garnet structure, showing edge sharing with two tetrahedra (I) and two octahedra (II). The cationic sites have been omitted.

trend between the distortions of tetrahedra and eight-coordinated sites, ascribed to the  $(\text{O–O})_1$  edge sharing of two tetrahedra with an eight-coordinated site (Fig. 2). Even if no detailed explanation of the behavior of these Si-bearing garnet phases can be proposed, the simultaneous presence of such different characteristics, at least in terms of geometrical characteristics, can be assumed to play a main role, as above evidenced for the variation of cell parameters.

### Infrared Spectra

$\text{Ca}_3\text{Sn}_{2+x}\text{Si}_{1-x}\text{Ga}_2\text{O}_{12}$ . According to the origin of the bands, these IR spectra (Fig. 3) may be more or less arbitrarily divided into four regions:  $950\text{--}800$ ,  $750\text{--}600$ ,  $500\text{--}300$ , and  $300\text{--}30 \text{ cm}^{-1}$ .

$950\text{--}800 \text{ cm}^{-1}$  region: The intensity of these bands decreases with increasing  $x$  values, and they disappear completely for  $x = 1$ : their assignment to the antisymmetric stretch ( $\nu_3$ ) of the  $\text{SiO}_4$  tetrahedron is straightforward. They may be considered as internal vibrations of the  $\text{SiO}_4$  tetrahedron, since the other coordinated groups ( $\text{GaO}_4$ ,  $\text{SnO}_4$ ,  $\text{SnO}_6$ ) give significantly lower frequencies and thus are not able to induce

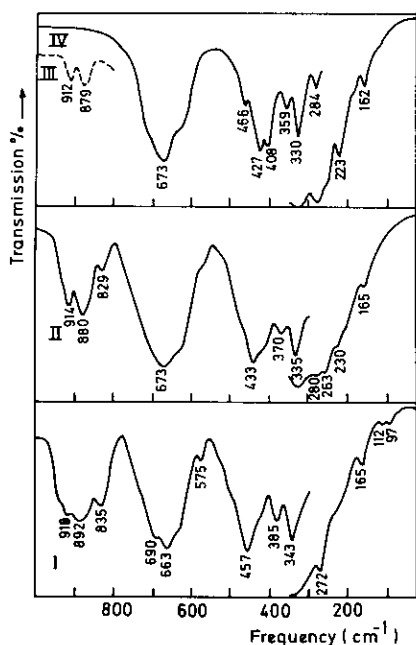


Fig. 3. IR spectra of selected compositions of  $\text{Ca}_3\text{Sn}_{2+x}\text{Si}_{1-x}\text{Ga}_2\text{O}_{12}$  phases: (I)  $\text{Ca}_3\text{Sn}_2\text{SiGa}_2\text{O}_{12}$ ; (II)  $\text{Ca}_3\text{Sn}_{2.5}\text{Si}_{0.5}\text{Ga}_2\text{O}_{12}$ ; (III)  $\text{Ca}_3\text{Sn}_{2.95}\text{Si}_{0.05}\text{Ga}_2\text{O}_{12}$  (high frequency region only); (IV) " $\text{Ca}_3\text{Sn}_3\text{Ga}_2\text{O}_{12}$ ." The break at  $350\text{--}300\text{ cm}^{-1}$  is of instrumental origin (grating spectrometer; 2 mgr in KBr discs above; interferometer; 6 mgr in polyethylene discs below  $350\text{--}300\text{ cm}^{-1}$ ).

important vibrational interactions. The overall pattern of these bands is progressively modified with increasing  $x$  values, but this is easily explained by the fact that the  $(\text{SiO}_4)$  groups are progressively "diluted" in the structure when  $x$  increases. For  $x = 0$ , vibrational interactions between near-neighbor  $\text{SiO}_4$  groups are possible and, from this point of view, the situation is more or less similar to that of a pure silicate garnet: the spectrum is approximately that predicted by the factor group splitting (three  $T_{1u}$ , IR-active modes); for increasing values of  $x$ , the average distance between  $\text{SiO}_4$  groups increases, the  $\text{SiO}_4\text{--SiO}_4$  vibrational interactions are progressively suppressed and, eventually, the number of bands is given by the site group ( $S_4$ ) splitting alone (two modes only). This is illustrated by the spectrum of the composition  $\text{Ca}_3\text{Sn}_{2.95}\text{Si}_{0.05}\text{Ga}_2\text{O}_{12}$  (Fig. 3III), whereas the

$\text{Ca}_3\text{Sn}_{2.5}\text{Si}_{0.5}\text{Ga}_2\text{O}_{12}$  composition is an example of an intermediate situation. The  $\text{SiO}_4$  bands remain fairly broad in the whole series of solid solutions. The origin of the relative broadness or sharpness of some spectra will be discussed later on.

$750\text{--}600\text{ cm}^{-1}$  region. The antisymmetric stretching vibrations of  $\text{GaO}_4$  tetrahedra are known to occur in this spectral region (9, 10). According to the factor group analysis, we expect a triplet in this region (this triplet is effectively observed in the IR spectrum of the garnets  $\text{Ln}_3\text{Ga}_5\text{O}_{12}$  (9)), but we observe only one strong band with one or two shoulders (depending on the  $x$  value): this is to be ascribed to the disordered distribution of several cations (Ga, Si and/or Sn) over the tetrahedral sites. Owing to the scarcity of compounds containing  $\text{SnO}_4$  tetrahedra, we have no reference data about the vibrational frequencies of these groups, but they may be roughly estimated by comparison with the vibrational behavior of  $\text{TiO}_4$  and  $\text{GeO}_4$  tetrahedra: in the IR spectrum of  $\text{Ba}_2\text{TiO}_4$  and  $\text{Ba}_2\text{GeO}_4$ , the antisymmetric vibrations of  $\text{TiO}_4$  and  $\text{GeO}_4$  groups are observed in the  $750\text{--}700\text{ cm}^{-1}$  (stretching) and  $400\text{--}300\text{ cm}^{-1}$  (bending) regions (10). The corresponding vibrations of  $\text{SnO}_4$  tetrahedra are thus expected to lie at slightly lower frequencies. In the IR spectrum of the actual solid solutions, we do not observe specific bands of the  $\text{SnO}_4$  tetrahedra: their frequencies are probably very similar to those of the  $\text{GaO}_4$  tetrahedra, with, as a consequence, a practically complete mixing of both  $\text{GaO}_4$  and  $\text{SnO}_4$  antisymmetric stretching vibrations.

$500\text{--}300\text{ cm}^{-1}$  region: In this region, definite assignments are very difficult, if not impossible, for the following reasons. If we consider the oversimplified scheme of internal vibrations, we may expect at least four types of vibrations in this region: some of the bending vibrations of the  $\text{SiO}_4$  tetrahedra, the bending vibrations of  $\text{GaO}_4$  and  $\text{SnO}_4$  tetrahedra, and the stretching motions of the  $\text{SnO}_6$  octahedra. Since in addition all the IR-active modes belong to the same  $T_{1u}$  representation, all these vibrations may in-

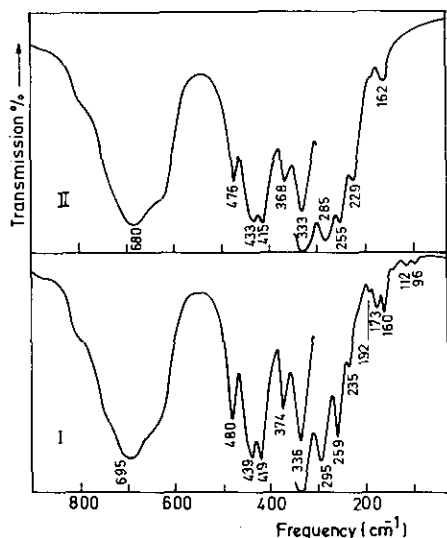


FIG. 4. IR spectra of  $\text{Ca}_3\text{Sn}_{2+x}\text{Ge}_{1-x}\text{Ga}_2\text{O}_{12}$  phases: (I)  $x = 0$ ; (II)  $x = 0.50$ .

teract, thus leading to complex, nonlocalized motions. An additional difficulty comes from the occurrence of several different cations statistically distributed over the tetrahedral sites. This contributes to the complexity of the vibrations, and to the broadness of the bands.

Low frequency region (below  $300\text{ cm}^{-1}$ ): Little can be said about this spectral region. The systematic occurrence of bands (or at least shoulders) near  $280$ ,  $230$  and  $165\text{ cm}^{-1}$  suggests their assignment to translations of the  $\text{Ca}^{2+}$  cation.

$\text{Ca}_3\text{Sn}_{2+x}\text{Ge}_{1-x}\text{Ga}_2\text{O}_{12}$ .  $800\text{--}600\text{ cm}^{-1}$  region: Contrary to the vibrational behavior of Si-bearing garnets, no specific band of the  $\text{GeO}_4$  stretching vibrations can be seen in the IR spectra of these solid solutions (Fig. 4). We observe only a broad absorption (with ill-defined shoulders), whose main maximum is slightly displaced towards lower frequencies when Ge is progressively replaced by Sn. This is easily explained by the fact that the  $\text{GeO}_4$ ,  $\text{SnO}_4$ , and  $\text{GaO}_4$  anti-symmetric stretching frequencies are not very different and are thus strongly coupled.

$500\text{--}30\text{ cm}^{-1}$  region: As previously stated, no definite assignment can be proposed for

this region, but an interesting feature is the sharpness of the spectra, which is much greater than that of the Si-bearing solid solutions. This point will be considered under the heading "Discussion."

### Raman Spectra

$\text{Ca}_3\text{Sn}_{2+x}\text{Si}_{1-x}\text{Ga}_2\text{O}_{12}$ . One of the most evident features of these spectra (Fig. 5) is their great similarity in the  $600\text{--}100\text{ cm}^{-1}$  region: there are just two strong bands (plus a few very weak ones), whose frequency is shifted toward lower frequencies with increasing values of  $x$ . No definite assignments can be proposed for these bands.

In contrast, important modifications (better illustrated in Fig. 6) are observed in the  $1000\text{--}600\text{ cm}^{-1}$  region:

(i) The weak bands of the  $1000\text{--}800\text{ cm}^{-1}$  region disappear progressively when Si is replaced by Sn: their assignment to stretching vibrations of the  $\text{SiO}_4$  tetrahedra is straightforward.

(ii) The broad band near  $753\text{ cm}^{-1}$  in the

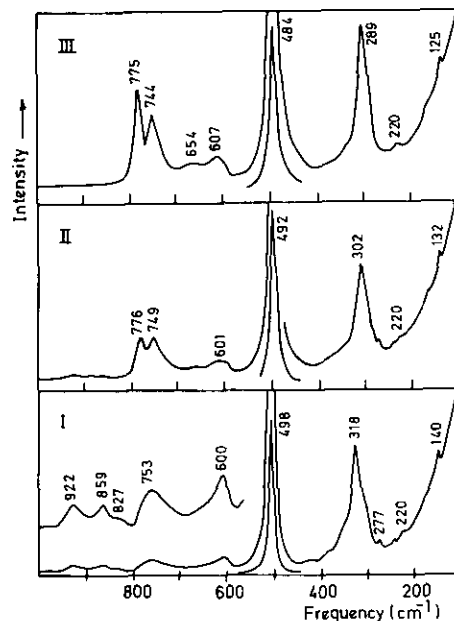


FIG. 5. Raman spectra of  $\text{Ca}_3\text{Sn}_2\text{SiGa}_2\text{O}_{12}$ : (I),  $\text{Ca}_3\text{Sn}_2\text{Si}_0.5\text{Ga}_2\text{O}_{12}$  (II), and  $\text{Ca}_3\text{Sn}_{2.95}\text{Si}_{0.05}\text{Ga}_2\text{O}_{12}$  (III).

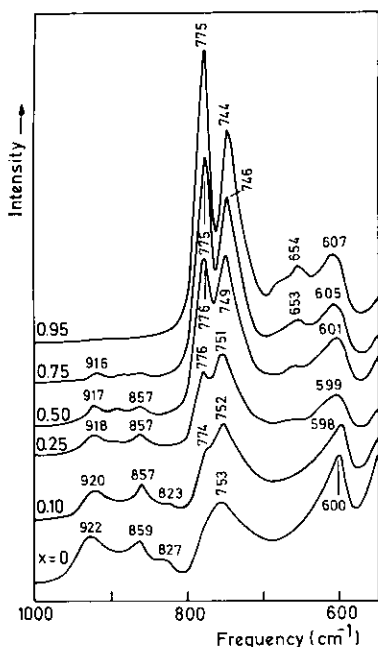


FIG. 6. Raman spectra of  $\text{Ca}_3\text{Sn}_{2+x}\text{Si}_{1-x}\text{Ga}_2\text{O}_{12}$  solid solutions in the  $1000\text{--}600\text{ cm}^{-1}$  region.

spectrum of the Si end-member ( $x = 0$ ) is assigned to a stretching vibration of the  $\text{GaO}_4$  tetrahedra, possibly the  $\nu_1$  totally symmetric mode ( $A_{1g}$  representation): this vibration has been observed at  $770$ ,  $767$ , and  $753\text{ cm}^{-1}$  in the Raman spectrum of  $\text{Yb}_3$ ,  $\text{Lu}_3$ , and  $\text{Gd}_3\text{Ga}_5\text{O}_{12}$  garnets, respectively (11, 12). But the most interesting feature of these spectra is the early appearance (for  $x = 0.10$ ; in fact, already visible for  $x = 0.05$ ), followed by the rapid growing, of a new band at  $775\text{ cm}^{-1}$ . This behavior strongly suggests its assignment to the  $\nu_1$  mode of  $\text{SnO}_4$  tetrahedra.

(iii) The remaining broad bands in the  $700\text{--}600\text{ cm}^{-1}$  region are assigned to anti-symmetric stretching motions of  $\text{GaO}_4$  tetrahedra (band near  $600\text{ cm}^{-1}$ , with an approximately constant intensity) and  $\text{SnO}_4$  tetrahedra (near  $650\text{ cm}^{-1}$ , missing for  $x = 0$ ; intensity increasing with the  $x$  values).

$\text{Ca}_3\text{Sn}_{2+x}\text{Ge}_{1-x}\text{Ga}_2\text{O}_{12}$ . The medium and low frequency spectra (Fig. 7) are rather similar to those of the Si-bearing solid solu-

tions, with the two very strong peaks near  $500$  and  $300\text{ cm}^{-1}$ . A significant difference is the occurrence, in the Ge end-member, of several weak, more or less sharp bands, which are apparently missing in the Si end-member (in fact, they are probably too weak and too broad to be observed: see "Discussion"). The high frequency part of the spectra exhibit a peculiar behavior (Fig. 8).

Two relatively sharp peaks ( $808$  and  $757\text{ cm}^{-1}$ ) are observed in the spectrum of the Ge end-member. They are assigned to the symmetric stretch  $\nu_1$  of the  $\text{GeO}_4$  and  $\text{GaO}_4$  tetrahedra, respectively. When Ge is progressively replaced by Sn, the following changes are observed:

$x = 0.25$ : the existing bands are slightly broadened and shifted towards lower frequencies, and a small hump is observed near  $780\text{ cm}^{-1}$

$x = 0.50$ : the preceding hump has grown to a weak band at  $777\text{ cm}^{-1}$ , which corresponds to the frequency of the band assigned to the  $\text{SnO}_4$   $\nu_1$  mode in the Si-bearing solid solutions

$x = 0.75$ : the new band, at  $775\text{ cm}^{-1}$ , is now largely predominant, whereas the band assigned to  $\text{GeO}_4$  is reduced to a weak shoulder

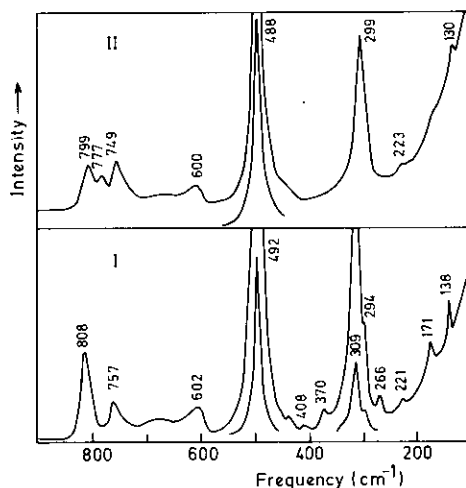


FIG. 7. Raman spectra of  $\text{Ca}_3\text{Sn}_2\text{GeGa}_2\text{O}_{12}$  (I) and  $\text{Ca}_3\text{Sn}_{2.5}\text{Ge}_{0.5}\text{Ga}_2\text{O}_{12}$  (II).



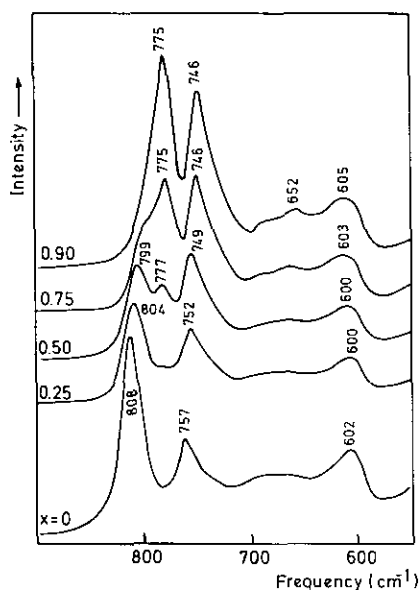


FIG. 8. Raman spectra of  $\text{Ca}_3\text{Sn}_{2+x}\text{Ge}_{1-x}\text{Ga}_2\text{O}_{12}$  solid solutions in the  $900\text{--}600\text{ cm}^{-1}$  region.

$x = 0.90$ : the relative intensity of the  $775\text{ cm}^{-1}$  band is still greater; the band assigned to  $\text{GeO}_4$  has disappeared.

This latter spectrum is very similar to that of the  $\text{Ca}_3\text{Sn}_{2.95}\text{Si}_{0.05}\text{Ga}_2\text{O}_{12}$  garnet, and it is clear that the  $775\text{ cm}^{-1}$  band must be assigned to the  $\nu_1$  mode of  $\text{SnO}_4$  tetrahedra.

This series of spectra, with a late appearance of the  $\text{SnO}_4$  band and a premature disappearance of the  $\text{GeO}_4$  band, is a typical example of mixed vibrational behavior, with either one-mode or two-modes vibrational behavior as a function of composition. This is to be correlated with the similarity of the  $\text{GeO}_4$  and  $\text{SnO}_4$  frequencies, whereas the large difference between the  $\text{SiO}_4$  and  $\text{SnO}_4$  frequencies leads to systematic two-modes behavior in the whole series of garnets  $\text{Ca}_3\text{Sn}_{2+x}\text{Si}_{1-x}\text{Ga}_2\text{O}_{12}$ .

The high-frequency assignments are summarized in Table III.

## Discussion

### Tetrahedral Coordination of $\text{Sn}^{4+}$

As stated in the introduction, the tetrahedral coordination of  $\text{Sn}^{4+}$  in its oxygen com-

pounds may be considered as exceptional, with only two types of known occurrences: the isotypic compounds  $\text{K}_4\text{SnO}_4$  and  $\text{Na}_4\text{SnO}_4$  (1), and the impure garnets " $\text{Ca}_3\text{Sn}_3\text{Fe}_2\text{O}_{12}$ " and " $\text{Ca}_3\text{Sn}_3\text{Ga}_2\text{O}_{12}$ " (3, 4) recently reinvestigated as a part of our work on the system  $\text{CaO}\text{--}\text{SnO}_2\text{--}\text{TiO}_2\text{--}\text{Fe}_2\text{O}_3$  (2) or of the system  $\text{Ca}_3\text{Sn}_{2+x}\text{Si}(\text{Ge})_{1-x}\text{Ga}_2\text{O}_{12}$  (this paper). It is thus interesting to discuss the reasons (or at least some of the reasons) of this peculiar behavior.

First of all, the preference of  $\text{Sn}^{4+}$  for octahedral sites is not the result of a peculiar electronic configuration (as is the case for some transition elements): it is a consequence of the relatively large value (0.55) of the ratio  $r_{\text{ion Sn}^{4+}}/r_{\text{ion O}^{2-}}$  (to be compared with the 0.26 figure of the  $r_{\text{ion Si}^{4+}}/r_{\text{ion O}^{2-}}$  ratio). This is supported by the fact that the tetrahedral coordination of  $\text{Sn}^{4+}$  is more frequent in its sulfur compounds (13). It may be inferred, at least as a working hypothesis, that in solid solutions of oxygen compounds, the introduction of tetrahedrally coordinated  $\text{Sn}^{4+}$  will be possible only if the tetrahedral sites of the host compounds are large enough to accommodate the  $\text{Sn}^{4+}$  ions without too large a distortion of the structure.

This seems to be supported by the actual data on the garnet structure. To the best of our knowledge, there is no reported

TABLE III  
SUMMARY OF THE HIGH FREQUENCY ASSIGNMENTS

Infrared spectra	
918–912, 892–879, 835–829 $\text{cm}^{-1}$ :	$\nu_3$ $\text{SiO}_4$
690–663 $\text{cm}^{-1}$ :	mixed $\nu_3$ $\text{GeO}_4$ + $\text{GaO}_4$ + $\text{SnO}_4$ vibrations
Raman spectra	
922–916, 859–857, 827–823 $\text{cm}^{-1}$ :	$\nu_1$ + $\nu_3$ $\text{SiO}_4$
808–799 $\text{cm}^{-1}$ :	$\nu_1$ $\text{GeO}_4$ ( $A_{1g}$ ) in $\text{Ca}_3\text{Sn}_{2+x}\text{Ge}_{1-x}\text{Ga}_2\text{O}_{12}$ solid solutions
777–774 $\text{cm}^{-1}$ :	$\nu_1$ $\text{SnO}_4$ ( $A_{1g}$ ) in all solid solutions with $x \neq 0$
757–744 $\text{cm}^{-1}$ :	$\nu_1$ $\text{GaO}_4$ ( $A_{1g}$ ) in all solid solutions
654–652 $\text{cm}^{-1}$ :	$\nu_3$ $\text{SnO}_4$ in Sn-rich solid solutions only
607–598 $\text{cm}^{-1}$ :	$\nu_3$ $\text{GaO}_4$ in all solid solutions

case of tetrahedrally coordinated  $\text{Sn}^{4+}$  in silicate garnets ( $r_{\text{Si}^{4+}}: 0.26 \text{ \AA}$ ). We are actually investigating the possibility of tetrahedral Ge–Sn replacement in suitable garnet germanates ( $r_{\text{Ge}^{4+}}: 0.39 \text{ \AA}$ ). So far, only two pairs of compositions have been investigated by X-ray diffraction, namely  $\text{Sr}_3\text{Y}_2\text{Ge}_{3-x}\text{Sn}_x\text{O}_{12}$  ( $x = 0$  and  $0.5$ ) and  $\text{Na}_2\text{CaSn}_{2+x}\text{Ge}_{3-x}\text{O}_{12}$  ( $x = 0$  and  $0.5$ ). With respect to the pure garnet phase ( $x = 0$ ), both Ge–Sn substituted compositions exhibit a small increase of the unit cell parameter, indicating the occurrence of some Ge–Sn replacement; but they exhibit also a number of additional diffraction peaks, showing that they are well outside the region of homogeneous solid solutions. The precise limit is still to be determined, but we may roughly estimate, from the variation of the unit cell parameter, a maximum value of  $x$  of  $0.2$  for  $\text{Na}_2\text{CaSn}_{2+x}\text{Ge}_{3-x}\text{O}_{12}$ , and of  $0.05$  only for  $\text{Sr}_3\text{Y}_2\text{Ge}_{3-x}\text{Sn}_x\text{O}_{12}$  solid solutions. These low limits are to be compared with the  $x = 0.95$  value observed when most of the tetrahedral sites are occupied by the  $\text{Ga}^{3+}$  ion ( $r_{\text{ion}}: 0.47 \text{ \AA}$ ).

It is clear that additional experiments are needed to check this trend.

Another point (raised by a reviewer) is the exclusive localization of the  $\text{Ga}^{3+}$  cations on the tetrahedral sites, instead of a distribution  $(\text{Ga}, \text{Sn})_{\text{tetra}} \leftrightarrow (\text{Ga}, \text{Sn})_{\text{octa}}$ . The possibility of such a distribution cannot be neglected if we consider that the tetrahedral ionic radii are not very different for  $\text{Ga}^{3+}$  ( $0.47 \text{ \AA}$ ) and  $\text{Sn}^{4+}$  ( $0.55 \text{ \AA}$ ). However, we know a large number of oxygen compounds with tetrahedrally coordinated  $\text{Ga}^{3+}$  ( $\text{LiGaO}_2$ ,  $\text{CaGa}_2\text{O}_4$ ,  $\text{LiGaGeO}_4$ ,  $\text{GaPO}_4$ , etc., see, e.g., Ref. (13)), whereas (as stated in the introduction) the tetrahedral coordination of  $\text{Sn}^{4+}$  is really exceptional.

From this experimental basis, we may conclude that the relative preferences of  $\text{Sn}^{4+}$  and  $\text{Ga}^{3+}$  for tetrahedral sites are drastically different, and cannot be deduced merely from a comparison of the ionic radii: the electronic structure must play an important role in this matter.

### Vibrational Spectra

*Compared vibrational behavior in the high frequency parts of the Raman and infrared spectra.* We have already noticed that, if  $\text{SiO}_4$  stretching vibrations can be observed in both IR and Raman spectra, discrete bands which can be assigned to stretching vibrations of  $\text{SnO}_4$  tetrahedra are never observed in the IR spectrum, whereas such bands are easily evidenced in the Raman spectrum of  $\text{Ca}_3\text{Sn}_{2+x}\text{Si}_{1-x}\text{Ga}_2\text{O}_{12}$  solid solutions. The situation is still more complicated for the  $\text{Ca}_3\text{Sn}_{2+x}\text{Ge}_{1-x}\text{Ga}_2\text{O}_{12}$  solid solutions: in the IR spectrum, the contributions of the three types of tetrahedral groups ( $\text{SnO}_4$ ,  $\text{GeO}_4$ , and  $\text{GaO}_4$ ) are mixed in a single broad, asymmetric absorption, whereas discrete bands are observed, at least for some compositions in the Raman spectrum.

This can be explained by the different symmetry properties of these vibrations.

Let us consider (as an approximation) the existence of internal stretching modes of the  $\text{SiO}_4$ ,  $\text{GeO}_4$ ,  $\text{GaO}_4$  and  $\text{SnO}_4$  tetrahedra.

In the IR spectrum, and according to the factor group analysis (14), the stretching vibrations of each type of tetrahedral group lead to  $3 T_{1u}$  modes.

For the higher  $\text{SiO}_4$  frequencies, the interactions with the lower  $\text{SnO}_4$  or  $\text{GaO}_4$  frequencies are small, and discrete  $\text{SiO}_4$  bands are observed in the spectra.

But for the  $\text{GeO}_4$ ,  $\text{SnO}_4$ , and  $\text{GaO}_4$  tetrahedra, whose stretching frequencies are of the same order of magnitude, we should have in the same spectral range either six ( $\text{SnO}_4 + \text{GaO}_4$ ) or nine ( $\text{GeO}_4 + \text{SnO}_4 + \text{GaO}_4$ ) vibrational frequencies which all belong to the same representation  $T_{1u}$ .

This leads to strong vibrational interactions, and the individual frequencies coalesce into a broad, asymmetric absorption.

The situation is different in the Raman spectrum: for a pure compound, the tetrahedral groups should give six Raman-active stretching vibrations, but they are distributed over three different representations (1

$A_{1g} + 2 E_g + 3 T_{2g}$ ). Among these, the most important one is the totally symmetric mode  $A_{1g}$  which, in the approximation of tetrahedral internal modes, is issued from the symmetric stretching mode  $\nu_1$  of the tetrahedron. It is interesting for the following reasons:

(i) The corresponding motion is limited to a simple symmetric displacement of the oxygen atoms only (all cations are necessarily at rest during this type of vibration).

(ii) For a given tetrahedral group, it is the only stretching vibration of this class

(iii) It is expected to give a reasonably strong Raman peak. For these reasons, the probability of vibrational interactions between different tetrahedral groups is much smaller than for the IR-active vibrations, and it should be possible to observe a specific band for each tetrahedral group, provided the individual frequencies of these groups are not too similar.

This is well illustrated by the Raman spectra of the solid solutions  $\text{Ca}_3\text{Sn}_{2+x}\text{Si}_{1-x}\text{Ga}_2\text{O}_{12}$ , with individual  $\text{SiO}_4$ ,  $\text{SnO}_4$ , and  $\text{GaO}_4$   $\nu_1$  frequencies in the whole series of solid solutions, and on the other hand the solid solutions  $\text{Ca}_3\text{Sn}_{2+x}\text{Ge}_{1-x}\text{Ga}_2\text{O}_{12}$ , for which individual  $\text{GeO}_4$  and  $\text{SnO}_4$   $\nu_1$  vibrations are observed only for a limited range of compositions, probably because of the similarity of their individual frequencies.

*Origin of the two strong Raman peaks near 500 and 300  $\text{cm}^{-1}$ .* For a pure compound, the factor group analysis predicts the existence of three totally symmetric  $A_{1g}$  vibrations. One of these, located in the high frequency part of the spectrum, is generally assigned to the  $\nu_1$  mode of the tetrahedral group (as far as this vibration can be considered as an internal mode). The two Raman peaks near 500 and 300  $\text{cm}^{-1}$  may be tentatively assigned to the two remaining  $A_{1g}$  modes, on the basis of their great intensity (though this is not a definitive argument). Since the cations are at rest during these vibrations, their frequency is essentially determined by the different cation–oxygen bonding forces, the sum of which gives the

overall restoring force determining the vibrational frequency.

If one of these bonds is much stronger than the others, its contribution to the overall restoring force is predominant, and the vibration may be considered (at least as a first approximation) as an internal mode: this is the case of the  $\nu_1$  mode of the tetrahedral group discussed previously. But for the 500 and 300  $\text{cm}^{-1}$  bands under discussion, there is no prevailing “local” restoring force: this would explain why no specific cationic influence can be observed on these frequencies.

*Broadness of some spectra.* We have already noticed the following features:

(i) The bands assigned to the stretching vibrations of the  $\text{SiO}_4$  tetrahedra are broad in both IR (Fig. 3) and Raman spectra (Fig. 6) of the solid solutions  $\text{Ca}_3\text{Sn}_{2+x}\text{Si}_{1-x}\text{Ga}_2\text{O}_{12}$ .

(ii) For the end-member compositions, the diffuseness of the spectra decreases in the sequence  $\text{Ca}_3\text{Sn}_2\text{SiGa}_2\text{O}_{12}$ , “ $\text{Ca}_3\text{Sn}_2\text{SnGa}_2\text{O}_{12}$ ,” and  $\text{Ca}_3\text{Sn}_2\text{GeGa}_2\text{O}_{12}$ , this latter composition giving sharp bands, at least below 600  $\text{cm}^{-1}$ . This appears clearly by comparison of Figs. 3I, 3IV, and 4I for the IR spectra, 5I and 7I for the Raman spectra.

These results can be explained by considering the following points:

(i) The occurrence of two (or several) different cations statistically distributed over the tetrahedral sites (as is the case for all compositions investigated in this paper) must induce some broadening of the vibrational spectrum. This is a classical consequence of disorder phenomena.

(ii) Our results show that the smallest broadening is observed for the smallest difference between the ionic radii of the tetrahedral cations, namely Ge (0.39 Å) and Ga (0.47 Å) in  $\text{Ca}_3\text{Sn}_2\text{GeGa}_2\text{O}_{12}$ ; in contrast, the greatest diffuseness is observed for the greatest difference between the ionic radii, Si (0.26 Å) and Ga in  $\text{Ca}_3\text{Sn}_2\text{SiGa}_2\text{O}_{12}$ . This should induce a greater distortion of the oxygen sublattice and an accordingly broader distribution of the vibrational frequencies.

As expected, the broadness of the bands is still greater for the intermediate solid solution  $\text{Ca}_3\text{Sn}_{2.5}\text{Si}_{0.5}\text{Ga}_2\text{O}_{12}$ , with three different cations on the tetrahedral sites (Fig. 3II).

(iii) An additional cause of broadness should be considered in the specific case of  $(\text{SiO}_4)$  vibrations: the average size of the tetrahedral voids is probably too large for the small Si cation, and this should also contribute to the broadness of the  $\text{SiO}_4$  bands, particularly in the range of Si-poor compositions.

## References

1. R. MARCHAND, Y. PIFFARD, AND M. TOURNOUX, *Acta Crystallogr. Sect. B* **31**, 511 (1975).
2. B. CARTIE, F. ARCHAIMBAULT, J. CHOISNET, A. RULMONT, P. TARTE, AND I. ABS-WURMBACH, *J. Mater. Sci. Lett.*, **11**, 1163 (1992).
3. B. V. MILL', *Dokl. Akad. Nauk SSSR* **165**, 555 (1965).
4. S. GELLER, *Z. Kristallogr.* **125**, 1 (1967).
5. R. D. SHANNON, *Acta Crystallogr. Sect. A* **32**, 751 (1976).
6. C. C. PHAM, J. CHOISNET, AND B. RAVEAU, *Bull. Acad. R. Belg.* **61**, 473 (1975).
7. J. ZEEMANN, *Beitr. Mineral. Petrogr.* **8**, 180 (1962).
8. F. C. HAWTHORNE, *J. Solid State Chem.* **37**, 157 (1981).
9. N. T. McDEVITT, *J. Opt. Soc. Am.* **59**, 1240 (1969).
10. P. TARTE, *Mém. Acad. R. Belg.* **35**, 4a and 4b (1965).
11. JIN-JOO SONG, P. B. KLEIN, R. L. WADSACK, M. SELDERS, S. MROCKZKOWSKI, AND R. K. CHANG, *J. Opt. Soc. Am.* **63**, 1135 (1973).
12. R. L. WADSACK, J. L. LEWIS, B. E. ARGYLE, AND R. K. CHANG, *Phys. Rev.* **3**, 4342 (1971).
13. E. PARTHE, "Cristallochimie des structures tétraédriques," Gordon & Breach, New York (1972).
14. D. M. ADAMS AND D. C. NEWTON, "Tables for Factor Group and Point Group Analysis" (Beckman, Ed.), Beckman-RIIC Limited, England (1970).